JOURNAL OF CATALYSIS **118**, 312–326 (1989)

Oxidative Dehydrogenation of 1-Butene on Iron Oxyhydroxides and Hydrated Iron Oxides

B. J. LIAW, D. S. CHENG, AND B. L. YANG[1]

National Central University, Chemical Engineering Department, Chung-Li, Taiwan, Republic of China

Received December 20, 1988; revised March 1, 1989

Steam, a component widely used in industrial dehydrogenation processes, has been found to play a role in converting the surfaces of iron oxide catalysts to hydroxyl surfaces. The catalytic properties of hydroxyl surfaces in the oxidative dehydrogenation of 1-butene have been studied in detail by investigating both pure iron oxyhydroxides and hydrated iron oxides. The following conclusions have been reached: (i) The hydroxyl surfaces are more active than their counterpart oxide surfaces in the oxidative dehydrogenation of 1-butene. (ii) The catalytic activities of iron oxyhydroxides are structure dependent. γ-FeOOH is much more active and selective than α-FeOOH. (iii) Steam has two compensating effects on iron oxide surfaces. It increases the activity by converting the surface to a more active hydroxyl form, but suppresses at the same time butene adsorption and reaction by a competitive adsorption.

INTRODUCTION

Iron oxide is known to be catalytically active for the dehydrogenation of hydrocarbons, especially of butene to butadiene (*1*) and ethylbenzene to styrene (*2*). Although extensive studies of the catalysts, including crystallographic dependency (*3–5*), effects of additives (*6, 7*), and active site characterizations (*5, 8, 9*) have been done in the oxidative dehydrogenation of butene, little has been known about the catalyst surface under reaction conditions. Most attempts to characterize the surface were made by using pure iron oxides as model catalysts. As is well known, the catalysts go through a redox cycle in the oxidative dehydrogenation of butene (*1, 4*). A certain degree of surface reduction is expected. Furthermore, steam is largely introduced into industrial reactors to minimize coking and to serve as a heat sink. The molar ratio of steam to hydrocarbon is usually on the order of 10 (*7, 10*). Under this high partial pressure of steam, the catalyst surface could be rich in hydroxyl group. Thermodynamically, α-Fe_2O_3 is the most stable phase of iron oxide in an oxidative atmosphere. However, α-Fe_2O_3 converts to FeOOH at 300°C if the pressure of steam reaches about 4000 atm (*11, 12*). It is then reasonable to expect that a certain degree of surface modification could occur under an intermediate pressure of steam, like 1 atm. Indeed, the affinity of water with pure iron oxide has been studied and reported in the literature (*13–15*). Chemisorption of water on iron oxide results in the formation of surface hydroxyl group as has been detected by IR (*13*). The amount of surface hydroxyl group is temperature dependent and is on the order of 10^{17}–$10^{18}/m^2$ on pure α-Fe_2O_3 after a desorption to 300°C (*14*). If the oxide surface is prereduced, the chemisorption of water is enhanced both in quantity and in adsorption strength (*15*).

The question is then whether the hydroxyl surface has any catalytic activity at all. If the hydroxyl surface is inactive, the introduction of steam would provide a negative effect on the catalyst by converting part of the surface to an inactive form. If the hydroxyl surface is active, it is then im-

---

[1] To whom correspondence should be addressed.

0021-9517/89 $3.00

portant to know how active the hydroxyl surface is, and how much contribution it makes in the overall performance of the catalyst.

To answer the above questions, we need to study the catalytic properties of hydroxyl surfaces. Two approaches have been taken. The first is to study model iron oxyhydroxides, including α-FeOOH, γ-FeOOH, and amorphous FeOOH. The surface of an iron oxyhydroxide is expected to be similar to that of a hydrated iron oxide because the hydration of iron oxide results in the formation of iron oxyhydroxide (*11*, *12*). Second, we also study the effect of steam on the catalytic performance of iron oxide, emphasizing mainly the chemical role of steam. The results of these two approaches will merge, and provide us with a better understanding of the hydroxyl surfaces of iron oxide catalysts under real operating conditions.

EXPERIMENTAL

Catalyst Preparation

The catalysts used in this study include amorphous FeOOH, α-FeOOH, γ-FeOOH, α-Fe_2O_3, and γ-Fe_2O_3. The amorphous iron oxyhydroxide was prepared by precipitation of an aqueous iron nitrate solution (0.1 *M*) with ammonia at a constant pH of 10.5 (*9*). The pH value of the solution was maintained by adding ammonia concentrate. After precipitation, the precipitate was filtered and washed repeatedly in cold and warm water several times until the filtrate showed a pH value close to 7. The final filtered cake was dried at about 80°C overnight and ground into a powder by a mortar and pestle. The obtained iron oxyhydroxide showed a dark brown color, appeared to be amorphous under X-ray diffraction, and had an irregular spherical shape under a transmission electron microscope (TEM). Upon calcination in air to 500°C, the iron oxyhydroxide converts to red α-Fe_2O_3. Reduction of α-Fe_2O_3 in a flowing stream of 1 vol% CO in CO_2 (LienHwa, unanalyzed) at 300°C produced black Fe_3O_4 (*16*). Reoxidation of Fe_3O_4 at 300°C in flowing O_2 (99.995%) resulted in the formation of yellow γ-Fe_2O_3. The completion of phase transformation was confirmed by X-ray diffraction and oxygen pulse tests (*3*).

γ-FeOOH was prepared following the method of Fricke and Zerrweck (*17*). Specifically, a solution of 30 g $FeCl_2 \cdot 4H_2O$ (Merck, GR) in 750 ml of water was added drop by drop into a solution of 42 g $(CH_2)_6N_4$ (Merck, GR) in 150 ml water to form the precipitate $Fe(OH)_2$. A solution of 10.5 g $NaNO_2$ (Merck, GR) in 150 ml water was then slowly added with continuous stirring. The mixture was heated to about 60°C and allowed to stand for 3 hr with occasional agitation to form γ-FeOOH. After that, the mixture was filtered and washed repeatedly in warm water and the final precipitate was dried at about 65°C overnight. The γ-FeOOH obtained showed an orange color and consisted of fine crystallites in a needle shape under TEM. The crystallographic structure of γ-FeOOH was confirmed by X-ray diffraction. α-FeOOH (99%), as well as additional samples of α-Fe_2O_3 (99.9%), were bought from Alfa U.S.A. as commercial chemicals.

Physical Characterization

X-ray diffraction (XRD) and Mössbauer effect spectroscopy (MES) were used for the phase identification (*18*). XRD was performed on a Rigaku Gagerflex diffractometer using either a Cu or a Mo target. The Mo radiation is more suitable for iron compounds due to the low degrees of fluorescence. MES was performed on a ASA S-600 Mössbauer spectrometer with ^{57}Co in Pd as the γ-ray source. A constant acceleration mode was always used and an iron foil was used as the standard. One part of sample powder was diluted by four parts of cellulose powder for MES studies.

For the specific surface area measurement, the conventional BET method was used with nitrogen as the adsorbate. The thermal stabilities of iron oxyhydroxides were studied by thermal gravimetric analyses in flowing nitrogen at a heating rate of 10°C/min from 50 to 750°C.

Catalytic Characterization

Both pulse reactions and steady-state reactions were performed to characterize the catalysts. The techniques used were conventional and have been reported previously (*6, 8*). In short, helium (99.995%, 30 ml/min) was used as the carrier gas for the pulse reaction and was purified on line by passing through a molecular sieve trap at liquid nitrogen temperature. The size of the 1-butene (99.3%) pulse was always 2.6×10^{18} molecules (±3%) and the amount of catalyst used was measured to maintain a constant surface area of 1.5 m^2 for a direct comparison. The catalyst was subjected to a 1-hr purging with helium before reaction. Unless otherwise stated, the purging was done at room temperature to avoid thermal decomposition of iron oxyhydroxide. After reaction, the products containing butadiene, CO_2, and butene isomers were first collected in a trap of Chromosorb W AW at liquid nitrogen temperature and then analyzed under gas chromatography (GC) using a separation column ($\frac{1}{4}$ in. × 5 m) packed with Chromosorb W AW coated with 20% dimethylsulfolane operated at 0°C, and a thermal conductivity detector operated at 100°C. Helium was used as the carrier gas (30 ml/min). After pulse reaction, the catalyst was heated to 500°C and the desorbed products were collected and analyzed. CO_2 was practically the only product detected from high-temperature desorption.

In steady-state reactions, a flow of premixed 1-butene in helium (5 vol% 1-butene) was first merged with an oxygen flow and a makeup helium flow and then conducted through a U-tube Pyrex reactor. The flows were controlled by mass flow controllers and a molar ratio of butene/O_2 = 1 was always maintained. Standard flow rates were He : O_2 : 1-butene = 58 : 2 : 2 ml/min. In case steam was needed, doubly distilled water was pumped by a metering pump into the system, passing an evaporator and a large-volume (1-liter) pressure damper to smooth out the pressure perturbation caused by the step action of the metering pump. Whenever steam was introduced, the flow rate of makeup helium was correspondingly reduced to maintain a constant total flow rate of 62 ml/min. The steam/1-butene molar ratio was kept at 10 at all times. The whole system was enclosed in an isothermal oven with forced convection at 120°C to avoid water condensation. Downstream from the reactor, the products were sampled on line by a six-way valve and GC-analyzed as in the pulse reaction.

RESULTS AND DISCUSSION

All catalysts used here have been examined by XRD and confirmed to be crystallographically pure. The results of BET surface area measurements are given in Table 1 along with the characteristic appearance of the catalysts. The water contents of iron oxyhydroxides have been measured by TGA. Crystalline α-FeOOH and γ-FeOOH samples have water contents slightly less than the stoichiometric amount, as can be seen in Table 1. In the amorphous iron oxyhydroxide, however, a significant amount of excess water was detected. Although $FeOOH \cdot 0.4H_2O$ might be a more realistic formula, we simply call it amorphous FeOOH in this discussion.

Iron Oxyhydroxide

We first studied the catalytic property of amorphous FeOOH by the pulse reaction of 1-butene. Table 2 gives the amounts of oxidation products from reactions at various temperatures. Indeed, butadiene was produced. The production of carbon dioxide was low at pulse temperatures but the later heating to 500°C resulted in a large amount of CO_2 desorption. The high-temperature CO_2 desorption was a result of both the total oxidation of irreversibly adsorbed butene and the desorption of the CO_2 preadsorbed before the reaction, which will be

TABLE 1

Some Properties of the Catalysts

Catalyst	BET surface area (m^2/g)	Shape of crystallite or particle	Color	Water content[a] (wt%)	Decomposition product
Amor. FeOOH	260	Irregular	Brown	15.3	α-Fe_2O_3
α-FeOOH	110	Needle	Yellow	8.0	α-Fe_2O_3
γ-FeOOH	210	Needle	Orange	8.2	γ-Fe_2O_3[b]
α-Fe_2O_3	38	Irregular	Red	—	—
γ-Fe_2O_3	38	Irregular	Yellow	—	—

[a] Theoretical water content of FeOOH is 10.1 wt%.

[b] Decomposition of γ-FeOOH at 300°C resulted in the formation of γ-Fe_2O_3; further calcination at higher temperatures converted γ-Fe_2O_3 to α-Fe_2O_3.

discussed in more detail later. Pulse reaction data presented in this paper have all been reproduced at least once. Typical data, instead of averaged data, are given here. Before we accept the results in Table 2 as proof of the activity of iron oxyhydroxide, we must consider that iron oxyhydroxide may not be thermally stable under all reaction conditions. Figure 1 shows the temperature dependency of the transformation of amorphous FeOOH to α-Fe_2O_3 as monitored by XRD. As can be seen in the figure, some crystallinity developed in the material after heating to 210°C, although no crystal pattern can be identified. After heating to 300°C, the pattern of α-Fe_2O_3 became detectable, and the phase transformation was completed after heating to 500°C. Then a possible explanation is that the catalytic activities given in Table 2 resulted from the α-Fe_2O_3 formed instead of amorphous FeOOH, since we know already that α-Fe_2O_3 is catalytically active. However, by comparing the activity of FeOOH with that of pure α-Fe_2O_3 in Table 3, we can no longer argue that α-Fe_2O_3 was the only active component, because it would then be difficult to explain why the pure α-Fe_2O_3 showed a lower activity. In other words, the results in Table 3 strongly indicate that amorphous FeOOH is indeed active for the production of butadiene. Also listed in Table 3 for comparison is the catalytic activity of γ-Fe_2O_3, the most active iron oxide known for this reaction.

Since the catalytic activity of amorphous FeOOH has been confirmed, it would be interesting to compare the FeOOH's of dif-

TABLE 2

Pulse Reactions of 1-Butene over Amorphous Iron Oxyhydroxide[a]

Reaction temp. (°C)	Catalyst amount (mg)	Products at pulse temp. (10^{16} molecules)		Later desorption to 500°C (10^{16} molecules)
		C_4H_6	$CO_2/4$	$CO_2/4$
100	5.8	9.2	0.3	9.4
210	6.0	90.7	0.6	12.5
300	5.6	135.0	4.2	26.2

[a] Size of 1-butene pulse was 2.6×10^{18} molecules.

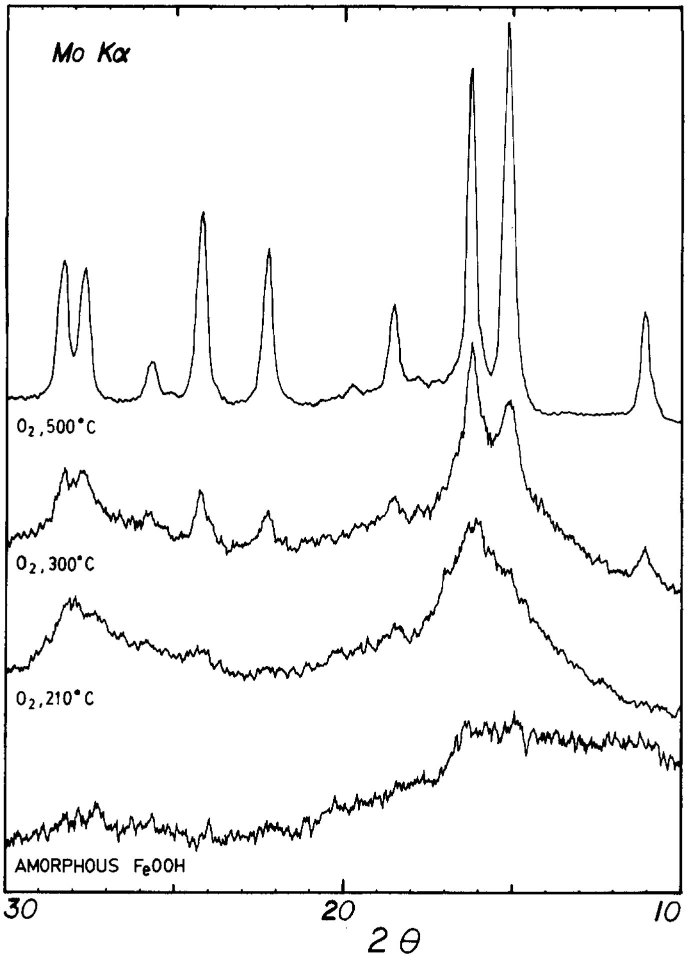

FIG. 1. X-ray diffraction spectra of amorphous iron oxyhydroxide after calcination at various temperatures.

TABLE 3

Comparison between Amorphous Iron Oxyhydroxide and Iron Oxide in Pulse Reaction of 1-Butene[a]

Reaction temp. (°C)	Catalyst	Catalyst amount[b] (mg)	Products at pulse temp. (10^{16} molecules)		Later desorption to 500°C (10^{16} molecules)
			C_4H_6	$CO_2/4$	$CO_2/4$
100	Amor. FeOOH	5.8	9.2	0.3	9.4
	α-Fe_2O_3	39.5	3.2	0.0	4.1
	γ-Fe_2O_3	39.0	46.2	0.0	2.3
210	Amor. FeOOH	6.0	90.7	0.6	12.5
	α-Fe_2O_3	40.0	44.9	0.3	9.0
	γ-Fe_2O_3	40.0	143.0	0.8	19.7

[a] Size of 1-butene pulse was 2.6×10^{18} molecules.

[b] Catalysts loaded had the same surface area of 1.5 m^2.

TABLE 4

Pulse Reactions of 1-Butene over Three Iron Oxyhydroxides at 210°C[a]

Catalyst	Catalyst amount[b] (mg)	Products at pulse temp. (10^{16} molecules)		Later desorption to 500°C (10^{16} molecules) $CO_2/4$
		C_4H_6	$CO_2/4$	
α-Fe_2O_3	13.7	3.1	0.3	21.9
γ-Fe_2O_3	7.0	45.3	1.3	19.2
Amor. FeOOH	6.0	90.7	0.6	12.5

[a] Size of 1-butene pulse was 2.6×10^{18} molecules.

[b] Catalysts loaded had the same surface area of 1.5 m^2.

ferent crystal structures. The crystalline FeOOH's studied were α-FeOOH and γ-FeOOH. As can be seen in Fig. 2, thermal gravimetric studies showed that crystalline FeOOH's went through clear phase transformations at temperatures from about 250 to 280°C, while on amorphous FeOOH, the decomposition occurred gradually and continuously, without a clear transformation point. Since the major phase transformation of crystalline FeOOH's occurs at temperatures above 250°C, the reaction temperature was chosen to be 210°C to avoid the major phase transformation. The catalytic activities of various FeOOH's were collected and given in Table 4. As can be seen in the table, α-FeOOH is much less active than γ-FeOOH and amorphous FeOOH.

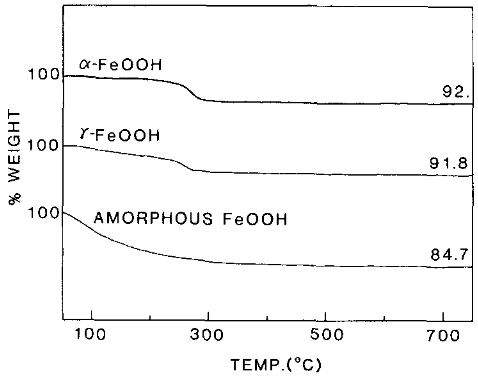

FIG. 2. Thermal gravimetric analyses of three iron oxyhydroxides.

It should be pointed out, however, that the results given in Tables 2 to 4 do not necessarily represent the activities of clean iron oxyhydroxide surfaces. Iron oxyhydroxides adsorb carbon dioxide in large amounts from the atmosphere. Stepwise thermal desorption of the CO_2 provides information on the amount and strength of CO_2 adsorption, as shown in Fig. 3. These measurements were done by equilibrating the samples to atmospheric air at room temperature for 1 day, followed by purging with helium at room temperature for 1 hr before the desorption measurement. The sample temperature was then raised stepwise. At each temperature, CO_2 was collected for 30 min and GC-quantified. A longer exposure of the samples to the atmosphere did not result in a larger adsorption of CO_2, indicating the attainment of equilibrium in 1 day. The heating employed in the thermal desorption, however, also caused the decomposition of iron oxyhydroxides to iron oxides at high temperatures. The strong adsorption of CO_2 indicates that the hydroxyl surface is basic in nature. CO_2 has been used as a probe molecule for the titration of surface basic sites (*19*). Carbon dioxide adsorbs on α-Fe_2O_3 too, but in a smaller amount, and the catalyst can be thermally cleaned before the pulse reaction. As was previously reported, the ad-

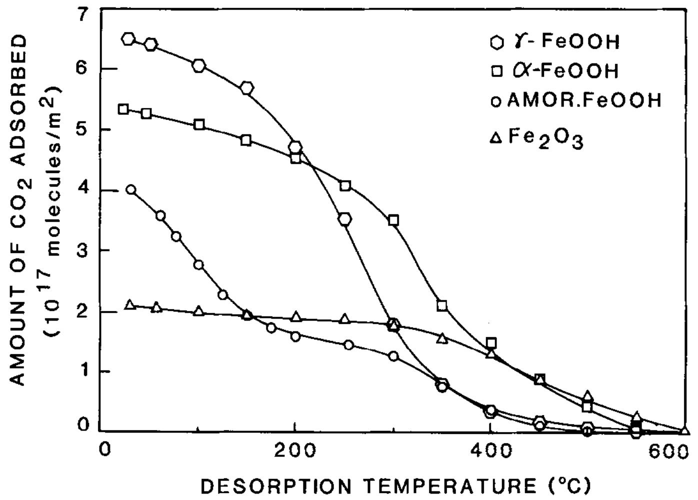

FIG. 3. Stepwise thermal desorption of CO_2 from passivated iron oxyhydroxides and α-Fe_2O_3.

sorbed CO_2 on iron oxide blocks the active site and suppresses butadiene production (*16*). Similar blocking on iron oxyhydroxides would also be expected. Indeed, purging iron oxyhydroxides at 210°C instead of at room temperature largely increased their activities as can be seen in Table 5. Flashing the catalyst in helium for 3 min to 210°C after the regular 1-hr room temperature purging resulted in a similar activity increase. This result indicates that the activities of clean iron oxyhydroxides should be exceptionally high, because by removing only 15–30% of preadsorbed CO_2, the butadiene activities increased two to three times. Also given in Table 5 is the activity of clean α-Fe_2O_3. Control experiments indicated that little CO_2 was left undesorbed after a helium purging at 300°C for 1 hr and at 500°C for 5 min. The high-temperature treatment made little change on the oxidation state of α-Fe_2O_3. Further treatment of

TABLE 5

Effect of Purging on the Performances of α-FeOOH, γ-FeOOH, and α-Fe_2O_3 at 210°C[a]

Catalyst	Purging conditions	Catalyst amount[b] (mg)	Products at pulse temp. (10^{16} molecules)	
			C_4H_6	$CO_2/4$
α-FeOOH	RT He 1 hr	13.7	3.1	0.3
	210°C O_2 1 hr RT He 1 hr	16.7	11.0	0.3
γ-FeOOH	RT He 1 hr	7.0	45.3	1.3
	210°C O_2 1 hr RT He 1 hr	8.9	103.0	0.6
α-Fe_2O_3	RT He 1 hr	40.0	44.9	0.3
	300°C He 1 hr 500°C He 5 min	39.5	97.0	—

[a] Size of 1-butene pulse was 2.6×10^{18} molecules.

[b] Catalysts loaded had the same surface area of 1.5 m^2.

TABLE 6

The Performances of Three Iron Oxyhydroxides in Steady-State Reactions at 250°C with and without Steam

Catalyst	Catalyst amount[a] (mg)	Without steam[b]				With steam[c]			
		Conversion		Selectivity		Conversion		Selectivity	
		Initial	Steady	Initial	Steady	Initial	Steady	Initial	Steady
α-FeOOH	236	0.12	0.04	0.79	0.68	0.12	0.03	0.80	0.63
γ-FeOOH	125	0.24	0.07	0.96	0.94	0.39	0.12	0.94	0.95
Amor. FeOOH	100	0.13	0.05	0.90	0.88	0.21	0.08	0.93	0.88

[a] Catalyst loaded had the same surface area.

[b] Flow rates He : O_2 : 1-butene = 58 : 2 : 2 ml/min.

[c] Flow rates He : H_2O : O_2 : 1-butene = 38 : 20 : 2 : 2 ml/min.

the catalyst in flowing oxygen at 300°C for 1 hr followed by the regular room temperature helium purging did not result in a significant activity change.

High activities of iron oxyhydroxides were also observed in steady-state reactions. Table 6 summarizes the performances of three iron oxyhydroxides in steady-state reactions, with and without steam. The reaction temperature was 250°C, and for a direct comparison the catalysts loaded had the same surface area. First, all three catalysts suffered from a decrease in activity with time and reached a quasi steady state in about 2 hr. The initial conversion and selectivity were measured after 15 min of reaction, and the steady-state values were taken after 3 hr on stream. The selectivity is defined as $C_4H_6/(C_4H_6 + CO_2/4)$ on a molar basis. The deactivation observed could be due to a gradual thermal decomposition of iron oxyhydroxide to iron oxide, or the formation of a carbonaceous deposit on the surface, or both. The formation of a carbonaceous deposit on the surface is possible because the reaction temperature was low. Steam is known to be capable of removing coke from the catalyst, but usually at temperatures much higher than 250°C. The coke-removing effect in this case is probably trivial. As can be seen in Table 6, the same deactivation pattern was also observed in the presence of steam. Previous studies on α-Fe_2O_3 found that the deactivation is strongly temperature dependent (*16, 20*). The higher the reaction temperature, the less the deactivation. Eventually, as the reaction temperature reached 350°C, the deactivation was no longer observed.

The decomposition of iron oxyhydroxide to iron oxide is also anticipated, and a higher degree of decomposition is anticipated in the absence than in the presence of steam. To study the effect of steam in stabilizing iron oxyhydroxide, we compared the Mössbauer spectra of amorphous FeOOH after heating in flowing oxygen and in a stream of 1 : 1 H_2O/N_2 mixture. The spectra are given in Fig. 4 and their key parameters, along with some literature data for comparison, are given in Table 7. First, all spectra showed an isomer shift between 0.3 and 0.4 mm/sec relative to iron, indicating that there were only ferric ions and no ferrous ions in the samples. The fresh amorphous FeOOH showed a clean central doublet at room temperature with no indication of hyperfine splitting. The quadrupole splitting of 0.65 mm/sec is in agreement with literature data (*38–40*). Upon heating to 200°C in air, the central doublet remained unchanged, but two tiny sets of magnetic hyperfine splitting also appeared. One, with a magnetic hyperfine field (*H*) 512 kOe, was α-Fe_2O_3; the other, showing an *H* of 374

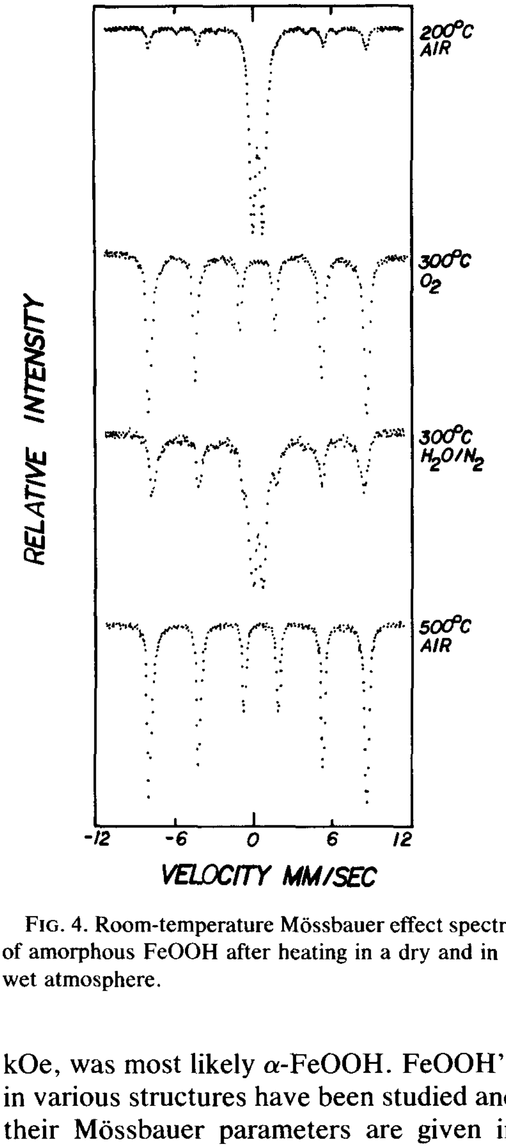

FIG. 4. Room-temperature Mössbauer effect spectra of amorphous FeOOH after heating in a dry and in a wet atmosphere.

kOe, was most likely α-FeOOH. FeOOH's in various structures have been studied and their Mössbauer parameters are given in Table 7. Among them, only α-FeOOH and δ-FeOOH exhibit a magnetic hyperfine splitting at room temperature. Their magnetic fields are, however, distinct enough to allow us to assign the second hyperfine splitting component in the 200°C sample to α-FeOOH. Upon calcination in air to 500°C, the material converted completely to α-Fe_2O_3, in agreement with the XRD results given in Fig. 1.

Interesting results were obtained when we compared the MES of amorphous FeOOH after heating to 300°C in flowing dry oxygen and that in a stream of 1 : 1 H_2O/N_2. While heating in dry oxygen resulted in a complete conversion to α-Fe_2O_3, as indicated by a clean six-line pattern with an *H* of 514 kOe, a strong central doublet with a quadrupole splitting of 0.68 mm/sec was still present after heating in H_2O/N_2. This central doublet can be attributed to the undecomposed amorphous FeOOH. α-Fe_2O_3 can also exhibit a central doublet due to the superparamagnetism in ultrafine particles (*22–24*). However, those ultrafine particles have to be dispersed on a high-surface-area support. No superparamagnetism has been observed on unsupported α-Fe_2O_3. Thus the central doublet in the 300°C H_2O/N_2-treated sample cannot be attributed to α-Fe_2O_3. Also, the quadrupole splitting of this central doublet is in agreement with that of amorphous FeOOH, but substantially smaller than that of superparamagnetic α-Fe_2O_3. Thus we come to the conclusion that steam does help in stabilizing iron oxyhydroxide from decomposition. The hyperfine splitting component in the H_2O/N_2-treated sample was α-Fe_2O_3. There is no indication of the formation of γ-Fe_2O_3. γ-Fe_2O_3 is in a cubic structure and exhibits no quadrupole splitting (*25, 26*).

The effect of steam is, however, temperature dependent. Heating amorphous iron oxyhydroxide at 400°C in either O_2 or H_2O/N_2 resulted in the same bulk conversion to α-Fe_2O_3.

As can be seen in Table 6, the presence of steam did increase the steady-state activities of γ-FeOOH and amorphous FeOOH by about 60%. Little effect on α-FeOOH was observed and the selectivities of all three catalysts were practically unaffected. The higher activities indicates that steam does help in preserving the hydroxyl surfaces from decomposition, and the hydroxyl surfaces exhibited better catalytic activities than their decomposition products, the oxides. Indeed, 660 mg of α-Fe_2O_3 which had about the same surface area resulted in little butadiene production under the same reaction conditions.

One interesting thing to note is the differ-

TABLE 7

Room Temperature Mössbauer Parameters of Amorphous FeOOH after Various Treatments in Comparison with Literature Data

Material	Treatment	QS[a] (mm/sec)	H[b] (kOe)	Phase component or reference
Amorphous FeOOH	Fresh	0.65	0	Amorphous FeOOH
	200°C air	0.69	0	Amorphous FeOOH
		0.6	374	α-FeOOH
		0.4	512	α-Fe_2O_3
	300°C O_2	0.4	514	α-Fe_2O_3
	300°C H_2O/N_2	0.68	0	Amorphous FeOOH
		0.5	500	α-Fe_2O_3
	400°C O_2	0.4	512	α-Fe_2O_3
	400°C H_2O/N_2	0.4	509	α-Fe_2O_3
	500°C air	0.4	513	α-Fe_2O_3
α-Fe_2O_3		0.48	515	(21)
α-Fe_2O_3/SiO_2		0.8–1.2	0	(22–24)
γ-Fe_2O_3		0	488–505	(25, 26)
α-FeOOH		0.5–0.6	0	(27–29)
		0.5–0.6	340–380	(30–32)
β-FeOOH		0.6–0.7	0	(28, 33)
γ-FeOOH		0.5–0.65	0	(34, 35)
δ-FeOOH		0.5–0.65	0	(36, 37)
		0.4	410	(36)
Amorphous FeOOH		0.54–0.62	0	(38–40)

[a] Quadrupole splitting.

[b] Magnetic hyperfine field.

ence between α-FeOOH and γ-FeOOH. It is well known that γ-Fe_2O_3 is much more active and selective than α-Fe_2O_3 for this reaction (3–5). A similar relation has also been found here between α-FeOOH and γ-FeOOH. Note that structure similarities exist between α-FeOOH and α-Fe_2O_3, as well as between γ-FeOOH and γ-Fe_2O_3. Oxygen atoms in both α-FeOOH and α-Fe_2O_3 form a hexagonal closest packing (41), while in γ-Fe_2O_3 and γ-FeOOH, oxygen atoms form a cubic closest packing (41). The decomposition of α-FeOOH results in the formation of α-Fe_2O_3, while that of γ-FeOOH results in the formation of γ-Fe_2O_3.

Possible reasons for the structure dependency in iron oxides have been discussed in the literature (4, 5). It has been proposed that a ferric ion in a tetrahedral site could be more active than that in an octahedral site (1, 5). γ-Fe_2O_3 has three-eights of its ferric ion siting in the tetrahedral sites, while all ferric ions in α-Fe_2O_3 are in octahedral sites (41). This is, however, not supported by our results on α-FeOOH and γ-FeOOH. Although γ-FeOOH is much more active and selective than α-FeOOH, both of them have only octahedral ferric ions (41).

The energetics of butadiene formation and the chemical properties of the reaction intermediates on both α-Fe_2O_3 and γ-Fe_2O_3 have been studied (1, 5, 8). It is found that the formation and desorption of butadiene occurs at a significantly lower temperature on γ-Fe_2O_3 than on α-Fe_2O_3, indicating a lower activation energy for the production of butadiene on γ-Fe_2O_3. A higher activity on γ-Fe_2O_3 than on α-Fe_2O_3 therefore results. Furthermore, butadiene precursors on α-Fe_2O_3 are easily attacked by gas-phase oxygen, resulting in a degradation into CO_2 production. Butadiene precursors on γ-

Fe_2O_3 are, however, insensitive to gas-phase oxygen; thus a higher selectivity to butadiene results. It would be very informative if we could make a similar comparison between α-FeOOH and γ-FeOOH. Unfortunately, this is prohibited by the fact that iron oxyhydroxide surfaces are severely poisoned by CO_2 adsorbed from the atmosphere, and the surface cannot be effectively cleaned without causing a decomposition of the material. Nevertheless, a rough measurement of the butadiene formation on a passivated γ-FeOOH indicated a desorption temperature very close to that on γ-Fe_2O_3 (*42*).

The high activity and selectivity of amorphous FeOOH is also interesting. As can be seen in Fig. 1, the amorphous FeOOH decomposes to α-Fe_2O_3. There is no indication that the peculiar performance of amorphous FeOOH can be linked to the γ-FeOOH structure. Particles of the amorphous FeOOH showed irregular spherical shapes under TEM, while γ-FeOOH crystallites were needle shaped. The high activity of amorphous FeOOH can probably be attributed, however, to its high density of surface defects. Amorphous materials are known to have surfaces rich in structural defects, and correlations between active sites and point defects like vacancies have been reported (*43, 44*). Actually, the catalytic performance of α-Fe_2O_3 has been found to be dependent on crystallite size (*20*). As the crystallite size dropped from 14.5 to 2.5 nm, the selectivity to butadiene increased from 51 to 77% at 300°C. This crystallite size effect could also be explained as a result of variation in surface imperfection.

Effects of Steam on Iron Oxides

As mentioned earlier, steam is widely used in industrial dehydrogenation processes. In the presence of steam, the surface of iron oxide could be converted to a hydroxyl form to some degree. Since we have found the iron oxyhydroxide to be very active, it is interesting to see whether or not the hydroxylation of the iron oxide surface can improve the activity of the catalyst.

Table 8 compares the performances of α-Fe_2O_3 and γ-Fe_2O_3 with and without steam. Steam improved the performance of γ-Fe_2O_3, but caused a negative effect on that of α-Fe_2O_3. Let us look at the performance of γ-Fe_2O_3 first. Figure 5 gives a detailed comparison with and without steam. Without steam, the activity of γ-Fe_2O_3 dropped gradually and reached a steady state in about 2 hr. The selectivity also dropped, but only slightly. By the addition of steam, the activity was improved and no deactiva-

TABLE 8

Effect of Steam on the Performances of α-Fe_2O_3 and γ-Fe_2O_3

Catalyst	Reaction temp. (°C)	Catalyst amount (mg)	Without steam[a]				With steam[b]			
			Conversion		Selectivity		Conversion		Selectivity	
			Initial	Steady	Initial	Steady	Initial	Steady	Initial	Steady
α-Fe_2O_3[c]	300	1000	0.07	0.04	0.54	0.50	0.04	0.02	0.53	0.50
α-Fe_2O_3[c]	350	100	0.08	0.10	0.64	0.61	0.05	0.05	0.56	0.54
γ-Fe_2O_3	300	100	0.18	0.08	0.97	0.93	0.21	0.21	0.97	0.96

[a] Flow rates He : O_2 : 1-butene = 58 : 2 : 2 ml/min.

[b] Flow rates He : H_2O : O_2 : 1-butene = 38 : 20 : 2 : 2 ml/min.

[c] α-Fe_2O_3 bought from Alfa Co. (99.9%), calcined in air at 600°C for 24 hr, having a BET surface area of 12 m^2/g.

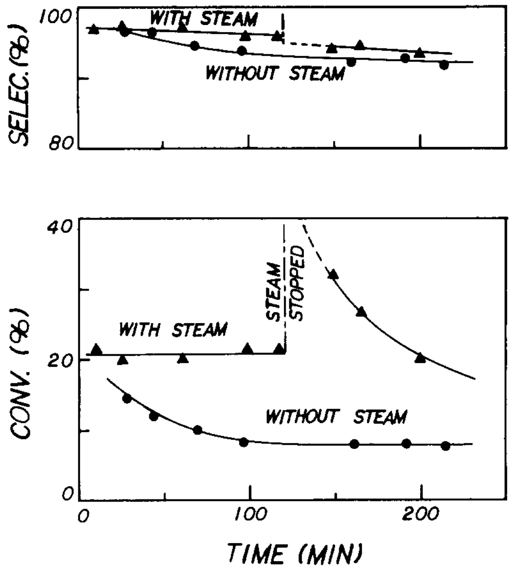

FIG. 5. Effect of steam on the performance of γ-Fe_2O_3 at 300°C.

tion was observed. The selectivity dropped slightly with time, but not as much as in the absence of steam. After 2 hr, the steam was stopped, while the total flow rate and the compositions of oxygen and butene remained unchanged. A drastic increase in activity was observed followed by a sharp and continuous drop. The large increase in activity after the steam was stopped can be explained as follows. The presence of steam has two compensating effects on the performance of γ-Fe_2O_3. One is to increase the activity by converting the catalyst surface to a hydroxyl form, but the adsorption of butene is resisted due to a competitive adsorption of water molecules. Water molecules also block the active site from butadiene production (*16*). Once the steam is stopped, the competing adsorption by steam no longer exists, but the surface has already been converted to a hydroxyl form; thus a large increase in activity resulted. Without a continuous supply of steam, the hydroxyl surface gradually decomposed back to an oxide surface, thus resulting in a continuous drop in activity. Figure 5 strongly suggests that the hydroxyl surface of γ-Fe_2O_3 is much more active than the dry oxide surface and is most likely the true surface responsible for the major activity of the catalyst under real operating conditions.

The question one would ask then is why the hydroxyl surface is more active. Although steam can be considered an oxidant by itself, the oxidation state of the catalyst is believed to be little affected by the presence of steam, since oxygen, a much stronger oxidant, was present in the reaction stream already. Furthermore, it has been reported that the activity of γ-Fe_2O_3 did not change even though the oxide was significantly reduced to γ-$Fe_2O_{2.8}$ (*4*). Thus the change in activity by adding steam cannot be attributed to the change in the oxidation state of the catalyst. The activity difference is not likely due to the decoking effect of the steam either, because the reaction temperature was low and no similar effect was observed on α-Fe_2O_3 at the same temperature.

As is well known, to increase the total reaction rate, the rate-limiting step must be accelerated. On γ-Fe_2O_3, the rate-limiting step in the oxidative dehydrogenation of butene has been confirmed to be the formation of an allylic intermediate by an allyl hydrogen abstraction (*4*). It is well accepted that 1-butene is adsorbed on a surface iron cation and loses one hydrogen to a nearby lattice oxygen (*1, 4*). When steam is present, the surface of iron oxide converts to a hydroxyl form via either hydroxylation or hydration as illustrated in Fig. 6. Hydroxylation involves a dissociative adsorption of water on a pair of surface O and Fe, while hydration requires breaking of an O–Fe bond and results in restructuring of the lattice. One major difference between the oxide surface and the hydroxyl surface is the degree of freedom of the surface oxygen. Oxygen in iron oxide is bonded to up to four iron cations and is in a rather fixed position. Upon hydroxylation of the surface, new OH groups are formed on the coordinatively unsaturated Fe. The only

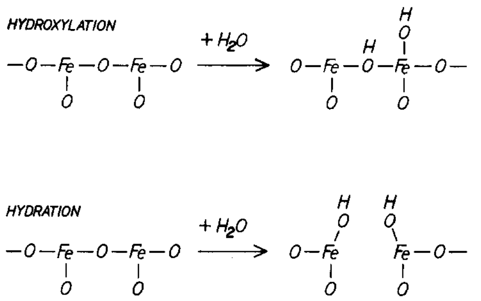

FIG. 6. Schematic models of surface hydroxylation and hydration on iron oxide.

link of oxygen in this OH group to the solid would be the single O–Fe bond. Thus a high degree of freedom in vibration and rotation is expected in this OH group. Upon hydration of the surface, some O–Fe bonds are replaced by O–H bonds. Oxygen of the hydroxyl group is again less linked to the solid and has more freedom in vibration and rotation than the surface oxygen in iron oxide. As for the dehydrogenation reaction, hydrogen is abstracted by the surface oxygen. Compared to an iron oxide surface, the hydroxyl surface has about a doubled density in oxygen available for hydrogen abstraction, and the oxygen has more freedom to physically meet the butene molecule to accelerate the hydrogen abstraction, and therefore the overall reaction.

Also, hydrogen is abstracted as a proton from the adsorbed butene molecule. A basic site is needed to accept the proton. The basicity of the surface oxygen has been reported to play a determinant role in the rate of allyl hydrogen abstraction in the oxidative dehydrogenation of butene and the selective oxidation of propylene on scheelite molybdate catalysts (*43*) and in the ammoxidation of propylene on promoted antimony oxides (*45*). By converting the surface of iron oxide to a hydroxyl form, the basic site density on the surface could be increased. The acid–base properties of metal oxides upon adsorption of water have been discussed by Morrison (*46*). The hydroxyl group can be considered a Brønsted base site (*19*). The large adsorption of CO_2 on iron oxyhydroxides (Fig. 3) also suggests the strong basicity of the hydroxyl surfaces. Thus the basicity of the hydroxyl surface provides an additional force in accelerating the hydrogen abstraction. Excess adsorption of water, however, results in the blocking of the surface by molecular water, and therefore in a decrease in activity.

As to the negative effect of steam on α-Fe_2O_3, the suppression of butene dehydrogenation due to the competitive adsorption of steam is probably stronger than the hydroxyl activation effect, thus resulting in a negative net effect.

CONCLUSION

In this study, we have demonstrated that iron oxyhydroxides are very active in the oxidative dehydrogenation of butene and their activities are strongly dependent on the crystallographic structure. Similar to the dependency found in iron oxides, γ-FeOOH is much more active and selective than α-FeOOH. Amorphous iron oxyhydroxide is also very active and selective, indicating a possible relationship between the active site and surface defects.

The iron oxyhydroxide surfaces are basic in nature and adsorb carbon dioxide in large amounts from the atmosphere. The surface could not be cleaned by thermal desorption without causing a decomposition of the material. Nevertheless, the surfaces of iron oxyhydroxides demonstrated strong activities regardless of the severe blocking of the active sites by CO_2 and H_2O.

On iron oxide, the presence of steam helps to increase the activity by converting the surface to a hydroxyl form, but suppresses the butene adsorption at the same time by a competitive adsorption. The hydroxyl surface has been found to be much more active than the oxide surface. This is attributed to both the basic nature of the hydroxyl surface and a higher degree of freedom of the oxygen in the surface hydroxyl group than that in iron oxide. The two compensating effects of steam resulted in a net improvement of the performance on γ-Fe_2O_3, but a suppression on α-Fe_2O_3.

The significance of this study is the finding that the hydroxyl surface is very active and is likely the real surface responsible for the major catalytic activity of iron oxide in the presence of steam. Therefore, basic characterization of the active sites should be made on the hydroxyl surfaces in addition to those on the oxide surfaces. Since steam is widely used with other oxide catalysts in other processes, like butene dehydrogenation on molybdates, butane dehydrogenation on chromates, ethylbenzene dehydrogenation on ferrites, and water-gas shift reaction on magnetite, a similar effect of steam in converting the surface to a hydroxyl form is expected and more understanding about the hydroxyl surfaces is needed. Indeed, in our preliminary study of the dehydrogenation of ethylbenzene, pretreating the iron oxide catalyst with steam before reaction greatly increased the initial activity of the catalyst (*47*).

ACKNOWLEDGMENTS

This work was supported by the National Science Council of the Republic of China. The authors are in debt to Professor H. H. Wei's group at Tamkang University, Tamsui, Taiwan, for their generous help in Mössbauer studies.

REFERENCES

1. Kung, H. H., and Kung, M. C., *in* "Advances in Catalysis" (D. D. Eley, P. W. Selwood, and Paul B. Weisz, Eds.), Vol. 33, p. 159. Academic Press, New York, 1985.
2. Lee, E. H., *Catal. Rev.* **8,** 285 (1973).
3. Misono, M., Nozawa, Y., and Yoneda, Y., *in* "Proceedings, 6th International Congress on Catalysis, London, 1976," (G. C. Bond, P. B. Wells, and F. C. Tompkins, Eds.), p. 386. The Chemical Society, London, 1977.
4. Misono, M., Sakata, K., Ueda, F., Nozawa, Y., and Yoneda, E., *Bull. Chem. Soc. Japan* **53,** 648 (1980).
5. Yang, B. L., Kung, M. C., and Kung, H. H., *J. Catal.* **89,** 172 (1984).
6. Kung, H. H., Kung, M. C., and Yang, B. L., *J. Catal.* **69,** 506 (1981).
7. Gibson, M., and Hightower, J. W., *J. Catal.* **41,** 420 (1976).
8. Yang, B. L., and Kung, H. H., *J. Catal.* **77,** 410 (1982).
9. Kung, M. C., Cheng, W. H., and Kung, H. H., *J. Phys. Chem.* **83,** 1737 (1979).
10. Welch, L. M., Croce, L. J., and Christmann, H. F., *Hydrocarbon Process.,* 131 (November 1978).
11. Schmalz, R. F., *J. Geophys. Rev.* **64,** 575 (1959).
12. Voigt, von R., and Bonn, G. W., *Neues Jahrb. Mineral. Monatsh.,* 89 (1981).
13. Rochester, C. H., and Topham, S. A., *J. Chem. Soc. Faraday Trans. 1* **75,** 872 (1979).
14. Morimoto, T., Nagao, M., and Tokuda, F., *Bull. Chem. Soc. Japan* **41,** 1533 (1968).
15. Lin, Z., Chen, Y., and Wu, X., *Surf. Sci.* **147,** 377 (1984).
16. Yang, B. L., Ph.D. thesis, Northwestern Univ., Evanston, IL, 1984.
17. Fricke, R., and Zerrweck, W., *in* "Handbook of Preparative Inorganic Chemistry" (G. Brauer, Ed.), Vol. 2, p. 1500. Academic Press, New York, 1965.
18. Hong, F., Yang, B. L., Schwartz, L. H., and Kung, H. H., *J. Phys. Chem.* **88,** 2525 (1984).
19. Knozinger, H., *in* "Advances in Catalysis" (D. D. Eley, P. W. Selwood, and Paul B. Weisz, Eds.), Vol. 25, p. 184. Academic Press, New York, 1976.
20. Yang, B. L., Hong, F., and Kung, H. H., *J. Phys. Chem.* **88,** 2531 (1984).
21. Kistner, O. C., and Sunyar, A. W., *Phys. Rev. Lett.* **4,** 412 (1960).
22. Yoshioka, T., Koezuka, J., and Ikoma, H., *J. Catal.* **16,** 264 (1970).
23. Gager, H. M., Hobson, M. S., and Lefelhocz, J. F., *Chem. Phys. Lett.* **15,** 124 (1972).
24. Malathi N., and Puri, S. P., *J. Phys. Soc. Japan* **31,** 1418 (1971).
25. Coey, J. M. D., and Khalafalla, D., *Phys. Status Solidi A* **11,** 229 (1972).
26. Armstrong, R. J., Morrish, A. H., and Sawatzky, G. A., *Phys. Lett.* **23,** 414 (1966).
27. Klissurski, D. G., and Bluskov, V. N., *Mater. Chem.* **5,** 67 (1980).
28. Yamamoto, N., Shinjo, T., Kiyama, M., Bando, Y., and Takada, T., *J. Phys. Soc. Japan* **25,** 1267 (1968).
29. Weaver, C. E., Wampler, J. M., and Pecuil, T. E., *Science* **156,** 504 (1967).
30. Shinjo, T., *J. Phys. Soc. Japan* **21,** 917 (1966).
31. Forsyth, J. B., Hedley, I. G., and Johnson, C. E., *J. Phys. C* **1,** 179 (1968).
32. Eissa, N. A., Sallam, H. A., Gomaa, S. Sh., Saleh, S. A., and Miligy, Z., *J. Phys. D* **7,** 2121 (1974).
33. Dezsi, I., Keszthelyl, L., Kuleawczuk, D., Molnar, B., and Fissa, N. A., *Phys. Status Solidi* **22,** 617 (1967).
34. Rossiter, M. J., and Hodgson, A. E. M., *J. Inorg. Nucl. Chem.* **27,** 63 (1965).

35. Takada, T., Kiyama, M., Bando, Y., Nakamura, T., Shinjo, M., Yamamoto, N., Endoh, Y., and Takaki, H., *J. Phys. Soc. Japan* **19,** 1744 (1964).

36. Du, Y. W., Zhang, Y. C., Jio, H. Z., Lu, H. X., Li, Z. Y., and Gu, B. X., *Acta Phys. Sin.* **28,** 773 (1979).

37. Povitskii, V. A., Makarov, E. F., Murashko, N. V., and Salugin, A. N., *Phys. Status Solid A* **33,** 783 (1976).

38. Okamoto, S., Sekizawa, H., and Okamoto, S. I., *in* "Reactivity of Solid" (J. S. Anderson, M. W. Roberts, and F. S. Stone, Eds.). Chapman and Hall, London, 1972.

39. Loseva, G. V., and Murashko, N. V., *Inorg. Mater.* **9,** 1301 (1973).

40. Saraswat, I. P., Vajpei, A. C., and Grag, V. K., *Indian J. Chem. A* **15,** 493 (1977).

41. Wells, A. F., "Structural Inorganic Chemistry," 5th ed. Clarendon Press, Oxford, 1984.

42. Liaw, B. J., Master thesis, National Central Univ., Chung-Li, Taiwan, 1987 (in Chinese).

43. Sleight, A. W., and Linn, W. J., *Ann. N.Y. Acad. Sci.* **272,** 22 (1976).

44. Sleight, A. W., *in* "Advanced Materials in Catalysis" (J. J. Burton and R. L. Garten, Eds.), pp. 181–208. Academic Press, New York, 1977.

45. Zhdan, P. A., Shepelin, A. P., Osipova, Z. G., and Sokolovskii, V. D., *J. Catal.* **58,** 8 (1979).

46. Morrison, S. R., *in* "Catalysis Science and Technology" (J. R. Anderson and M. Boudart, Eds.), Vol. 3, Ch. 4. Springer–Verlag, New York, 1982.

47. Yang, S. Y., Master thesis, National Central Univ., Chung-Li, Taiwan, 1987 (in Chinese).